Molecular dynamics calculation of the thermal conductivity of superlattices

Brian C. Daly and Humphrey J. Maris

Department of Physics, Brown University, Providence, Rhode Island 02906

K. Imamura and S. Tamura

Department of Applied Physics, Hokkaido University, Sapporo 060, Japan

We report on molecular dynamics studies of heat flow in superlattices. The computer simulations are performed using classical mechanics with periodic boundary conditions. The heat flow is in the direction normal to the layers. We have studied the variation of the conductivity with the repeat distance and the effect of interfacial roughness. We discuss the relation of these results to experimental data in the literature.

I. INTRODUCTION

Superlattices are structures composed of alternating layers of two materials that have nearly the same lattice parameter. Semiconductor superlattices have optical, electronic, and thermal properties that vary significantly from those of the bulk constituent materials. These novel properties have led to the use of superlattice structures in a number of applications, including semiconductor lasers[1] and thermoelectric devices.[2,3] The operation of these devices can be greatly affected by the thermal conductivity of the superlattice. For instance, the efficiency of a semiconductor laser is reduced when the active region of the device is at high temperature, and so a high thermal conductivity superlattice is preferred. On the other hand, the efficiency of a thermoelectric device is inversely proportional to the thermal conductivity, and so low thermal conductivity materials are preferable. The study of heat flow in a superlattice is also of interest from a fundamental perspective. The periodicity of the superlattice modifies the phonon dispersion relation. The effects of this modification on the lattice thermal conductivity have been studied by several authors,[4–6] but discrepancies between theoretical calculations and experimental values have not yet been resolved.

Measurements on Si/Ge (Ref. 7) and GaAs/AlAs (Ref. 8) superlattices have shown that the thermal conductivity in the direction perpendicular to the layers (growth direction) is reduced by as much as an order of magnitude compared to the conductivity of the bulk constituents. Part of the decrease in the thermal conductivity can be attributed to the reduction in the group velocity of phonons due to zone folding.[5] However, quantitative calculations show that this effect should lead to a thermal conductivity that decreases as the thickness of the layers making up the superlattice is increased within the range from one to ten monolayers. Experimental results for samples with layer thickness in this range have shown the opposite effect, as can be seen from the data of Capinski *et al.*[8] shown in Fig. 1, which show a monotonic increase in the thermal conductivity with increasing superlattice period. The disagreement between the zone-folding theory and the data may be due to interface effects,[9] but the extent to which interfacial roughness and other superlattice defects affect the experimentally measured thermal conductivity is not yet

known. In order to investigate the effects of the different superlattice parameters on the thermal conductivity in the growth direction, we have performed molecular dynamics simulations on a simple, classical model of a superlattice and present the results here.

II. MOLECULAR DYNAMICS SIMULATION

In this paper, we are primarily interested in achieving an understanding of the general characteristics of heat flow in superlattices, rather than performing quantitative calculations for any particular system. The parameters entering into the model are designed to provide a highly simplified model for heat flow in GaAs/AlAs superlattices. For these simulations we use a simple fcc lattice of atoms with nearest-neighbor harmonic and anharmonic interactions. Calculations based on a model of this type have been presented in papers by Maradudin and co-workers[10] and by Maris and Tamura.[11,12] The parameters that enter for this model are the atomic mass M, the lattice parameter a_0 (nearest-neighbor spacing is $a_0\sqrt{2}$), and the second and third derivatives of the interatomic potential which we will denote by β and β'. The potential energy between a pair of neighboring atoms is taken to be

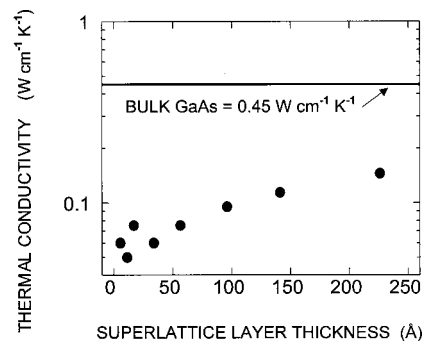$$V = \frac{1}{2}\beta(r - a_0\sqrt{2})^2 + \frac{1}{6}\beta'(r - a_0\sqrt{2})^3, \tag{1}$$

FIG. 1. Thermal conductivity of GaAs/AlAs superlattices at 300 K as a function of superlattice period as measured by Capinski *et al.* (Ref. 8) together with the value for bulk GaAs.

where r is the distance between the atoms.

To simulate GaAs, we select the value of the mass M to be the average of the atomic masses of Ga and As.[13] Thus the two-atom unit cell of GaAs is represented by a single atom in our simulation. The lattice parameter is then determined from the expression for the density:

$$\rho = \frac{M}{2a_0^3}. \tag{2}$$

This gives $a_0 = 2.24 \times 10^{-8}$ cm for GaAs. The bulk modulus B is equal to $2\beta/3a_0$. The experimental value of B is 7.6×10^{11} g cm^{-1} s^{-2}, and to give this correctly we choose $\beta = 2.557 \times 10^4$ g s^{-2}. It is straightforward to show that the Grüneisen parameter γ is given by the expression

$$\gamma = -\frac{\beta' a_0}{3\sqrt{2}\beta}. \tag{3}$$

This value of γ is the same for all phonon modes. One possibility would be to choose β' so that Eq. (3) is consistent with the value of γ as determined from thermal expansion measurements. However, in real GaAs there is a large variation in the value of γ between the different branches of the phonon spectrum. For example, the longitudinal acoustic modes have γ around 1, whereas some of the transverse modes have negative values of γ.[14] As a result, the γ calculated from thermal expansion would be smaller than the average of the magnitude of the γ's for the individual modes, and so choosing γ from thermal expansion would significantly underestimate the anharmonicity. Consequently, for the present, we arbitrarily choose $\beta' = -4.84 \times 10^{12}$ g cm^{-1} s^{-2}, so that Eq. (3) gives $\gamma = 1$.

For AlAs, the mass is chosen as the average of the atomic masses of Al and As. The lattice constant is chosen to be the same as that of GaAs. Since the bulk modulus of AlAs differs from that of GaAs by only a few percent, we choose β to have the same value as in GaAs. For simplicity, we also choose β' to have the same value.

One can consider a number of different approaches to the calculation of the thermal conductivity. For example, one could consider a sample that is in contact with hot and cold thermal reservoirs at opposite ends and then compute the heat flowing between the reservoirs. This was the method used by Payton, Rich, and Visscher in their seminal work on molecular dynamics simulations of heat flow in one-dimensional (1D) chains and 2D lattices.[15] Further calculations on 1D and 2D systems that followed this approach were made by Nishiguchi and co-workers.[16,17] Another possibility is to use the Green-Kubo formulation to calculate the thermal conductivity from the correlation function of thermal fluctuations in the system.[18–21] In our calculation, we have chosen to use the following method. We consider a sample of dimensions $3200 \times 20 \times 20$ atoms, with periodic boundary conditions applied in all three directions. We set up an initial temperature distribution of the form

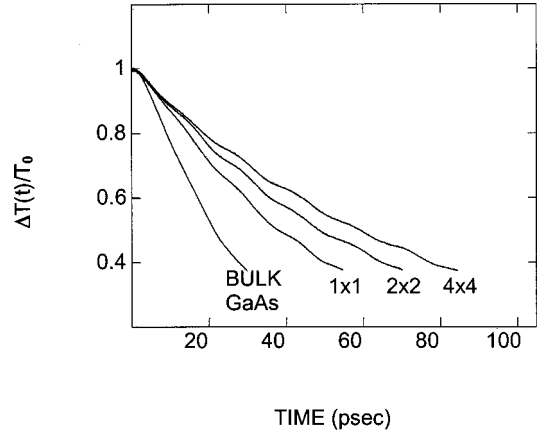$$T(x, t=0) T_0 + \Delta T_0 \cos(2\pi x/L_x), \tag{4}$$

FIG. 2. Computer simulation of the decay of a temperature distribution as a function of time. The mean temperature is 300 K. Results are plotted for the bulk GaAs lattice and for 1×1, 2×2, and 4×4 superlattices.

where L_x is the length of the lattice in the x direction and the magnitude ΔT_0 of the temperature perturbation is 10% of the base temperature T_0. The atoms of the lattice are assigned a random initial momentum based on a Maxwell distribution that corresponds to the local temperature $T(x, t=0)$. We then monitor the decay of the temperature perturbation as a function of time in order to determine the thermal conductivity. The position and momentum of the atoms are calculated as time progresses using a simple "leapfrog" algorithm.[22] At selected time intervals, we calculate the energy of each atom in the sample. We then find the average of the energy of the 20×20 atoms in the y-z plane with a given x coordinate, and from this average, we determine the temperature $T(x, t)$ as a function of x. We then determine the current magnitude $\Delta T(t)$ of the temperature perturbation by using the formula

$$\Delta T(t) = \frac{2}{L_x} \int_0^{L_x} T(x, t) \cos(2\pi x/L_x) dx. \tag{5}$$

Sample results for $\Delta T(t)/\Delta T_0$ are shown in Fig. 2.

These cooling curves exhibit a number of interesting features. First, we note that $\Delta T(t)$ contains a small-amplitude oscillation. When the temperature distribution is applied at $t=0$, a spatially varying thermal stress is set up. This excites the sample into a low frequency vibrational mode in which the atoms vibrate in the x direction. The vibrational energy associated with this motion makes a small contribution to the total energy, and this leads to an oscillatory contribution in $\Delta T(t)$. Neglecting this oscillation, we now try to analyze the cooling curve to determine κ. Based on Fourier's law, we expect that

$$\Delta T(t)/\Delta T_0 = \exp(-4\pi^2 Dt/L_x^2), \tag{6}$$

where D is the thermal diffusivity. If the value of D is chosen so as to give a fit at large t, we find that the fit based on Eq. (6) gives too high a cooling rate for small t. The reason for this discrepancy can be seen by examining the Green's function solution to the one-dimensional diffusion equation:

$$G(x,t) = \frac{1}{\sqrt{4\pi Dt}} \exp\left(\frac{-x^2}{4Dt}\right). \qquad (7)$$

This Green's function implies that at time t heat has flowed a distance of the order of $(4Dt)^{1/2}$. Thus the speed with which the heat moves is of the order of $(4D/t)^{1/2}$, which gives an infinite velocity at $t=0$. However, clearly heat can never travel faster than the phonon velocity v. One simple, but *ad hoc*, way to modify the Green's function to avoid this non-physical behavior is to replace $4Dt$ in Eq. (7) by the quantity

$$\frac{4Dtv^2t^2}{4Dt+v^2t^2}, \qquad (8)$$

where v is an average phonon velocity. Then, for small t, the distance that heat flows will be of the order of vt. With the use of this modified Green's function, it is straightforward to show that the temperature perturbation now decays according to the equation

$$\Delta T(t)/\Delta T_0 = \exp\left[-\frac{\pi^2}{L_x^2}\left(\frac{4Dv^2t^2}{4D+v^2t}\right)\right]. \qquad (9)$$

The molecular dynamics results for $\Delta T(t)/\Delta T_0$ are fit to this form using D and v as adjustable parameters. The value of κ is then calculated from the expression $\kappa = DC$, where C is the specific heat per unit volume of the lattice. Using this method, calculated values of κ for a particular $3200 \times 20 \times 20$ lattice do not vary by more than 10% when a different set of random initial momenta of the atoms in the lattice are used.

The simulations for which the results are presented in this paper were performed using personal computers with processor speeds of 600 MHz, and each took between 3 and 7 days to complete. Some tests on lattices of $6400 \times 20 \times 20$ atoms were performed on a Hitachi SR8000 supercomputer and took up to 16 h on that machine.

The time for $\Delta T(t)$ to decrease to a chosen fraction of its initial value increases as the square of the sample length L_x. Since the number of atoms in the simulation increases linearly with L_x, it follows that the time taken to run the simulation varies as L_x^3.

If the phonon mean free path Λ is longer than the length of the sample in the x direction, phonons can travel ballistically from the hot to the cold region. The time for the temperature perturbation to disappear would then be of the order of the length of the sample L_x divided by the sound velocity. Under these conditions, the time for the temperature distribution to decay does not provide information about the thermal conductivity. Thus, to obtain a correct value of κ, it is necessary for L_x to be significantly greater than Λ. To estimate Λ for bulk GaAs, we take the value of the conductivity κ calculated by the molecular dynamics simulation (see results given in next section) and then use the method of Stoner and Maris[23] to obtain Λ from κ. At 300 K this gives a value of 1200 Å. We compare this with the value of L_x, which is 7168 Å for a sample 3200 cells long. In Fig. 3, we show the results of an investigation of the variation of the calculated conductivity with sample length. We find that
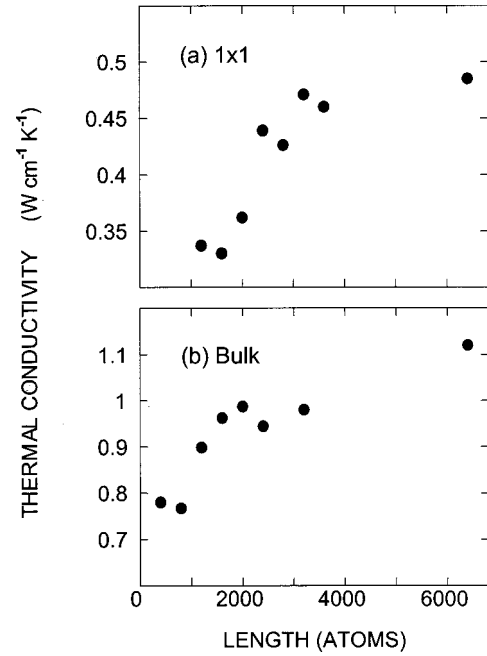

FIG. 3. Calculated thermal conductivity vs lattice length for (a) a 1×1 superlattice and (b) bulk GaAs. The temperature is 300 K.

even up to a length of 6400 cells, the value of κ has still not converged to a completely stable value. The difference in κ on going from 3200 cells to 6400 cells is less than 10%, but it should be noted that because of limitations on computer time, this is based on a single run on the larger sample.

We have also investigated the effect of increasing the lateral dimensions of the lattice from 20×20 to 40×40. For bulk GaAs at 300 K, the conductivity decreases by 0.6%, for the 1×1 superlattice κ decreases by 5.3%, and for the 1×1 superlattice with rough interfaces κ increases by 1.6%. Since these changes are small, we elected to use 20×20 in most of the simulations.

III. RESULTS

We have made calculations for a number of different GaAs/AlAs superlattices. The following calculations were all made for superlattices that were $3200 \times 20 \times 20$ atoms in size.

A. Isotopically pure superlattices

In this set of calculations, we set the mass of each GaAs unit by using the average isotopic mass in Ga, i.e., 69.7 amu. Results for κ as a function of superlattice repeat distance are plotted in Fig. 4, along with the results of computer simulations for bulk GaAs. The calculated conductivity of GaAs at 300 K is approximately twice the experimental value. This discrepancy is not surprising given the simplicity of our model. The conductivity of all of the superlattices we have studied is reduced compared to the bulk material, and for all but the largest repeat distances, this reduction is greater than
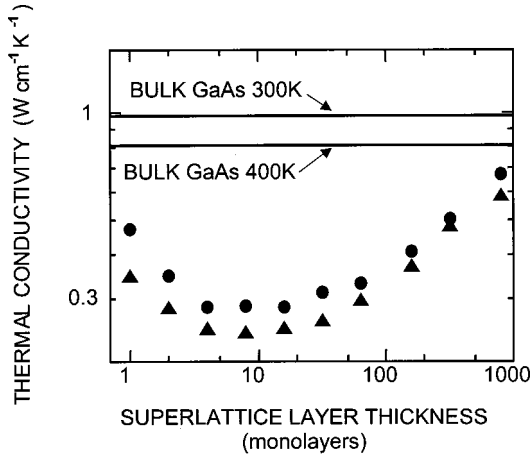
FIG. 4. Thermal conductivity as a function of superlattice period for 300 and 400 K. The solid circles (●) and triangles (▲) represent the thermal conductivity calculated for superlattices at 300 and 400 K, respectively. The solid lines represent the thermal conductivity calculated from simulations of bulk GaAs at the two temperatures.

a factor of 2. This is in reasonable agreement with the calculations of Ref. 5. For the longer period superlattices the decrease in κ relative to bulk GaAs is in reasonable agreement with experimental data. For example, the reduction for the 16×16 superlattice at 300 K is a factor of 3.5, compared to a reduction of 4.4 measured for a 17×17 sample.[8]

It is important to note the trends in the thermal conductivity as the repeat distance changes. At repeat distances larger than eight monolayers, the reduction factor is smaller the longer the period, as is found experimentally. For the short-period superlattices, however, the calculation gives a reduction factor that *increases* as the period becomes longer. This behavior has not been observed experimentally. It is seen, however, in the zone-folding calculations found in Refs. 5 and 6. The effect of the zone folding is a flattening of the phonon dispersion curve, which results in a lower phonon group velocity. This decrease in the group velocity of the heat-carrying phonons yields a reduction in thermal conductivity that increases with increasing period for short-period superlattices. Thus our calculation supports the hypothesis that zone folding is the dominant effect on κ in the short-period superlattices. We can therefore say that the short-period superlattices behave as a crystal with a modified phonon dispersion relation.

When the superlattice period is very long compared to the phonon mean free path, the thermal resistance of one period of the structure should be equal to the sum of the resistance of the layers of GaAs and AlAs plus the Kapitza resistance R_K (thermal boundary resistance) (Refs. 24–26) of the two interfaces. Thus the conductivity should approach a value κ such that

$$\frac{1}{\kappa} = \frac{1}{2\kappa_{\text{GaAs}}} + \frac{1}{2\kappa_{\text{AlAs}}} + \frac{R_K}{d}, \qquad (10)$$

where d is the thickness of one layer. When $d \to \infty$, this formula gives a conductivity $\kappa_\infty = 1.08$ W cm^{-1} K^{-1} at 300 K, using for κ_{GaAs} and κ_{AlAs} the results from the simulation. It

is evident from Fig. 4, however, that even for a layer thickness of 800 atoms the superlattice thermal conductivity has not reached this limit. (Note, however, that for this layer thickness there are only four layers in the sample.) Equation (10) gives a conductivity that increases as the period increases, as is seen in the simulations in the range of large layer thickness. The combination of the zone-folding effect for short periods, giving a conductivity decreasing with increasing period, and the conductivity increasing with period that occurs for long periods results in the conductivity minimum seen in Fig. 4. This minimum in the thermal conductivity was predicted by Simkin and Mahan.[6]

Also plotted in Fig. 4 are the molecular dynamics results at 400 K. Comparing the results at 300 and 400 K, we see that the rate of change of the thermal conductivity with temperature is affected by changes in the superlattice period. For the bulk and for the shortest-period superlattices, we find that $\kappa \propto T^{-n}$ where n is about 1 or slightly less than 1. A T^{-1} dependence is expected for the thermal conductivity of dielectric crystals when three-phonon processes are solely responsible for the finite phonon lifetime. The same temperature dependence is expected for short-period superlattices in which the phonon mean free path is very much longer than the period. This is because we can view such superlattices as crystals with a modified dispersion relation. Since the phonon lifetime is governed by three-phonon processes, the conductivity will still vary as T^{-1}. As the superlattice period increases, however, we see a general decrease in the dependence of κ on temperature. This behavior can be understood based on Eq. (10). The conductivities κ_{GaAs} and κ_{AlAs} both vary as T^{-1}, whereas the thermal boundary resistance at the interface between two different materials is expected to be independent of temperature for $T > \Theta_D$.[25,26] Thus, for a layer thickness such that Eq. (10) applies, it is to be expected that the conductivity of the superlattices will vary with temperature less rapidly than as T^{-1}.

B. Superlattices with natural isotope concentration

We also performed molecular dynamics calculations of the thermal conductivity of a set of GaAs/AlAs superlattices where the naturally occurring distribution of isotopic masses for Ga was used in order to determine the mass of the GaAs units. Note that since Al and As are isotopically pure, there is no variation in mass in the AlAs layers. The simulations were performed for a temperature of 300 K. The results are plotted in Fig. 5 along with the results for the perfect superlattices discussed in the previous section. While we find a 10% reduction in the thermal conductivity of the bulk GaAs, we see only a very small effect on the thermal conductivity of the 1×1 superlattice and essentially no effect on the thermal conductivity for any of the other superlattices.

While measurements of the effect of isotopic purity on the thermal conductivity of bulk and thin-film semiconductors can be found in the literature,[27–30] the thermal conductivity of superlattices with isotopically enriched layers has not yet been studied experimentally. Measurements on isotopically enriched Ge (Ref. 27), diamond (Ref. 28), and Si (Refs. 29 and 30) show increases in the room-temperature thermal con-
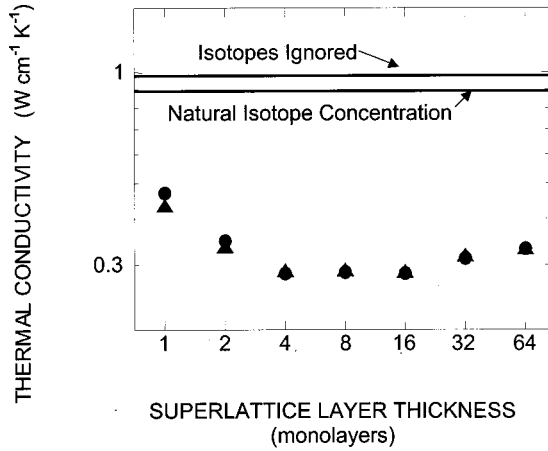
FIG. 5. Thermal conductivity vs superlattice period at 300 K. The triangles (▲) represent the calculated thermal conductivity for the cases where the natural isotope concentration is used, and the circles (●) represent the cases where the natural isotope concentration of Ga is ignored (isotopically pure). The solid lines represent the conductivity of bulk GaAs for the two cases.

ductivity of 30%, 50%, and 60%, respectively, over the same materials with natural isotope concentrations. The molecular dynamics calculation shows a considerably smaller effect for bulk GaAs. However, the magnitude of the mass disorder in GaAs is much less than in Ge, Si, and C. The rate of phonon scattering due to isotopes is proportional to the parameter Γ, which is given by the expression

$$\Gamma = \sum_i f_i (1 - M_i / M_0)^2, \tag{11}$$

where $M_0 = \sum_i f_i M_i$ and f_i is the fraction of atoms with mass M_i. The value of Γ for natural GaAs is 0.46×10^{-4}, whereas $\Gamma = 5.8 \times 10^{-4}$, 0.76×10^{-4}, and 2.0×10^{-4} for Ge, C, and Si, respectively. Thus a smaller isotope effect is expected in GaAs. Additionally, in C, for which Γ is larger than GaAs by a factor of only 1.7, account must be taken of the high Debye temperature (2000 K). At 300 K, the temperature is less than $\Theta_D/6$, and at temperatures much less than Θ_D we expect a greater effect of isotope scattering on the thermal conductivity. The rate of isotope scattering in GaAs/AlAs superlattices has been calculated by Tamura.[31] He finds that the isotope scattering rate of transverse phonons in a superlattice is higher than that of longitudinal phonons, but that both rates are lower than the rate in bulk GaAs. He also finds that both scattering rates decrease as the superlattice period increases.

C. Superlattices with interfacial roughness

In order to calculate the effects of interfacial roughness on heat flow in superlattices, we incorporated a very simple model of roughness into the simulation. For the last atomic monolayer of each superlattice layer, the mass of each atom was randomly assigned to be the mass of a GaAs atom or an AlAs atom, with a 50% probability of each. Measurements on GaAs/AlAs superlattices grown by molecular beam epitaxy (MBE) have shown that a transition region containing
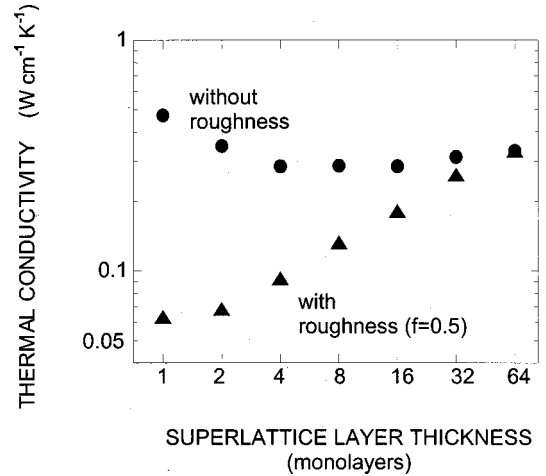

FIG. 6. Thermal conductivity vs superlattice period at 300 K. The triangles (▲) represent superlattices for which interfacial roughness is included. The circles (●) represent the perfect superlattices discussed in Sec. III A.

both superlattice constituents typically exists at the boundary between superlattice layers.[32,33] This region is usually about a monolayer in thickness. However, it must be noted that this rough region often takes the form of islands that have lateral dimensions of a few hundred angstroms. Since our lateral dimensions are smaller than these islands, it is not possible for us to simulate this sort of roughness at this time. We also note that since we are using periodic boundary conditions in all directions, the "random" roughness we have introduced at the interfaces is effectively repeated with a period of 20 atoms in the lateral directions.

The results of simulations performed for rough superlattices at 300 K are shown in Fig. 6 along with the results for the perfect superlattices discussed in Sec. III A. The results demonstrate that the introduction of the roughness at the interfaces reduces the thermal conductivity of the shortest period superlattices by almost an order of magnitude. As expected, this effect decreases with increasing superlattice period, and for the 64×64 superlattice, we find no significant effect on the thermal conductivity. It is interesting to note that the minimum value of κ discussed in Sec. III A is no longer evident in the rough superlattice data. That is to say, the thermal conductivity of these rough superlattices increases with increasing superlattice period over the entire range of periods. This sort of behavior is what has been seen experimentally. Thus it appears that interfacial roughness may account for the discrepancy between the calculated reduction in the superlattice thermal conductivity due to zone folding and the reduction observed in the experimental data.

We have also investigated the effects of different degrees of roughness at the superlattice interfaces. To do this, we considered a series of samples in which the probability f of an atom in the last monolayer of a GaAs layer being changed to an AlAs atom varied in the range between 0 and 0.5. The probability that an atom in the last AlAs layer was GaAs was also equal to f. We call f the roughness factor of the superlattice. The results of this test for a 1×1 and a 2×2 superlattice at 300 K are plotted in Fig. 7. As expected, the ther-
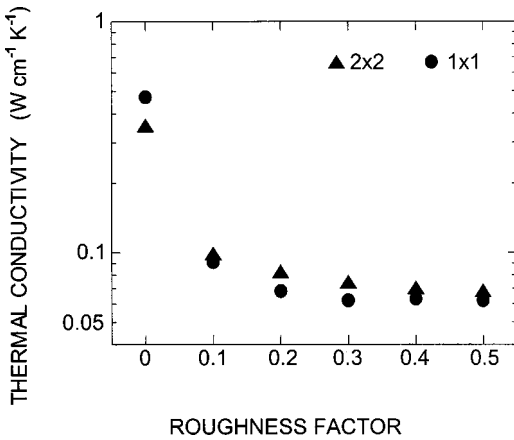
FIG. 7. Thermal conductivity vs roughness factor at 300 K. The circles (●) and the triangles (▲) represent the thermal conductivity calculated for the 1×1 and 2×2 superlattices, respectively. A roughness factor of 0.0 indicates that the calculation was performed for a perfect superlattice.

mal conductivity reduction increases with the increasing roughness factor. We see that even with only 10% roughness, the thermal conductivity is reduced by a factor of 4 for the 1×1 superlattice and 3 for the 2×2 superlattice.

The thermal conductivity of the superlattices with a roughness factor of 0.5 is replotted in Fig. 8 for 300 and 400 K. For the short-period superlattices, the temperature dependence of the thermal conductivity is significantly reduced compared with that of the perfect superlattices for which κ is plotted in Fig. 4. This decrease in temperature dependence is reasonable in light of the fact that the addition of roughness to the interfaces is expected to increase the thermal boundary resistance at each interface. The thermal boundary resistance is independent of temperature, so if the interfacial thermal

resistance becomes the dominant effect on the superlattice conductivity, a more temperature independent value of κ is expected.

Finally, we comment on the thermal conductivity of the $Al_{0.5}Ga_{0.5}As$ alloy. It is interesting to note that our model of a rough 1×1 superlattice with a roughness factor of 0.5 is essentially a binary alloy composed of 50% AlAs atoms and 50% GaAs atoms. From Figs. 4 and 8, we see that we have calculated a value of 0.98 $W\,cm^{-1}\,K^{-1}$ for the conductivity of GaAs and a value of 0.062 $W\,cm^{-1}\,K^{-1}$ for the conductivity of the $Al_{0.5}Ga_{0.5}As$ alloy. This reduction of a factor of ~16 is considerably larger than the reduction found experimentally, which is a factor of ~4.[34] The discrepancy is surprising since previous theoretical work on the thermal conductivity of semiconductor alloys[35,36] has predicted a reduction similar to that which was seen experimentally. Abeles[36] has calculated the thermal conductivity of semiconductor alloys using a model that incorporates phonon-phonon scattering as well as scattering from point defects. The defects limit the phonon lifetime in the alloy by means of their mass difference as well as their size difference. Aframowitz[34] has used this theory to obtain a reasonable fit to his measurements of the thermal conductivity of $Al_xGa_{1-x}As$ alloys.

IV. CONCLUSIONS

We have used the method of molecular dynamics on a classical fcc lattice model in order to study the lattice thermal conductivity of semiconductor superlattices. Our calculations of the reduction of the thermal conductivity of perfect superlattices compared with that of the bulk constituent materials are in good agreement with calculations based on the effect of Brillouin zone folding. With the addition of a simple model of interface roughness, we calculate a dependence of the thermal conductivity on superlattice period that is similar to that which has been seen experimentally. In the near future, we intend to use this molecular dynamics technique to investigate novel superlattice systems for which the thermal conductivity is of interest. Such simulations could serve as a guide for experimental work by assisting in the design of multilayer structures that have a thermal conductivity of a selected value. It should also be possible to perform simulations for more realistic models of the GaAs/AlAs system. To do this it would be necessary to use the real crystal structure and a significantly more complicated model for the harmonic and anharmonic interatomic forces. It would also be necessary to use a more sophisticated model for the interatomic forces at the interfaces. Such simulations would probably require at least 10 times more computer time than has been needed for the simulations reported in the present paper.
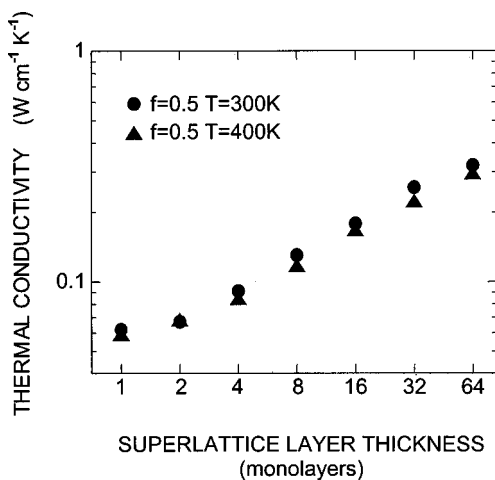

FIG. 8. Thermal conductivity vs superlattice period for rough superlattices. The circles (●) represent the calculated values at 300 K, the triangles (▲) represent the calculated values at 400 K.

[1] T. E. Sale, *Vertical Cavity Surface Emitting Lasers* (Research Studies Press, Taunton, Somerset, England, 1995).

[2] L. D. Hicks, T. C. Harman, and M. S. Dresselhaus, Appl. Phys. Lett. **63**, 3230 (1993).

[3] P. J. Lin-Chung and T. L. Reinecke, Phys. Rev. B **51**, 13 244 (1995).

[4] S. Y. Ren and J. D. Dow, Phys. Rev. B **25**, 3750 (1982).

[5] S. Tamura, Y. Tanaka, and H. J. Maris, Phys. Rev. B **60**, 2627 (1999).

[6] M. V. Simkin and G. D. Mahan, Phys. Rev. Lett. **84**, 927 (2000).

[7] S. M. Lee, D. G. Cahill, and R. Venkatasubramanian, Appl. Phys. Lett. **70**, 2957 (1997).

[8] W. S. Capinski, H. J. Maris, T. Ruf, M. Cardona, K. Ploog, and D. S. Katzer, Phys. Rev. B **59**, 8105 (1999).

[9] G. Chen, Phys. Rev. B **57**, 14 958 (1998).

[10] A. A. Maradudin, P. A. Flynn, and R. A. Coldwell-Horsfall, Ann. Phys. (N.Y.) **15**, 360 (1961).

[11] H. J. Maris and S. Tamura, Phys. Rev. B **47**, 727 (1993).

[12] S. Tamura and H. J. Maris, Phys. Rev. B **51**, 2857 (1995).

[13] By selecting the atomic mass to be the average of the masses of Ga and As, we find a lower value for the harmonic force constant β than was used in the fcc model of Ref. 5. In that paper, the authors selected the atomic mass to be the sum of the masses of Ga and As.

[14] S. Adachi, *GaAs and Related Materials* (World Scientific, River Edge, NJ, 1994).

[15] D. N. Payton, M. Rich, and W. M. Visscher, Phys. Rev. **160**, 706 (1967).

[16] N. Nishiguchi and T. Sakuma, J. Phys.: Condens. Matter **2**, 7575 (1990).

[17] N. Nishiguchi, N. Takahashi, and T. Sakuma, J. Phys.: Condens. Matter **4**, 1465 (1992).

[18] R. Kubo, J. Phys. Soc. Jpn. **12**, 570 (1957).

[19] S. Volz and G. Chen, Physica B **263−264**, 709 (1999).

[20] S. Volz and G. Chen, Phys. Rev. B **61**, 2651 (2000).

[21] S. Volz, J. B. Saulnier, G. Chen, and P. Beauchamp, Microelectron. J. **31**, 815 (2000).

[22] See, for example, R. P. Feynman, R. B. Leighton, and M. Sands, *The Feynman Lectures on Physics* (Addison-Wesley, Reading, MA, 1963) Vol. 1, Chap. 9, Sec. 6.

[23] R. J. Stoner and H. J. Maris, Phys. Rev. B **47**, 11 826 (1993).

[24] E. T. Swartz and R. O. Pohl, Rev. Mod. Phys. **61**, 605 (1989).

[25] D. A. Young and H. J. Maris, Phys. Rev. B **40**, 3685 (1989).

[26] R. J. Stoner and H. J. Maris, Phys. Rev. B **48**, 16373 (1993).

[27] T. H. Geballe and G. W. Hull, Phys. Rev. **110**, 773 (1958).

[28] L. Wei, P. K. Kuo, R. L. Thomas, T. R. Anthony, and W. F. Banholzer, Phys. Rev. Lett. **70**, 3764 (1993).

[29] W. S. Capinski, H. J. Maris, E. Bauser, I. Silier, M. Asen-Palmer, T. Ruf, M. Cardona, and E. Gmelin, Appl. Phys. Lett. **71**, 2109 (1997).

[30] T. Ruf, R. W. Henn, M. Asen-Palmer, E. Gmelin, M. Cardona, H.-J. Pohl, G. G. Devyatych, and P. G. Sennakov, Solid State Commun. **115**, 243 (2000).

[31] S. Tamura, Phys. Rev. B **56**, 12 440 (1997).

[32] R. F. Kopf, E. F. Schubert, T. D. Harris, and R. S. Becker, Appl. Phys. Lett. **58**, 631 (1991).

[33] T. Ruf, J. Spitzer, V. F. Sapega, V. I. Belitsky, M. Cardona, and K. Ploog, Phys. Rev. B **50**, 1792 (1994).

[34] M. A. Aframowitz, J. Appl. Phys. **44**, 1292 (1973).

[35] P. G. Klemens, Phys. Rev. **119**, 507 (1960).

[36] B. Abeles, Phys. Rev. **131**, 1906 (1963).